NJC

Accepted Manuscript

This is an *Accepted Manuscript*, which has been through the Royal Society of Chemistry peer review process and has been accepted for publication.

Accepted Manuscripts are published online shortly after acceptance, before technical editing, formatting and proof reading. Using this free service, authors can make their results available to the community, in citable form, before we publish the edited article. We will replace this *Accepted Manuscript* with the edited and formatted *Advance Article* as soon as it is available.

You can find more information about *Accepted Manuscripts* in the Information for Authors.

Please note that technical editing may introduce minor changes to the text and/or graphics, which may alter content. The journal's standard Terms & Conditions and the Ethical guidelines still apply. In no event shall the Royal Society of Chemistry be held responsible for any errors or omissions in this *Accepted Manuscript* or any consequences arising from the use of any information it contains.

ROYAL SOCIETY OF CHEMISTRY

www.rsc.org/njc

Superabsorbent Enhanced-Catalytic Core/Shell Nanocomposites Hydrogel for Efficient Water Decolorization

Rania E. Morsi[*] *and Radwa A. Elsalamony*

Egyptian Petroleum Research Institute, Cairo, 11727, Egypt

Abstract

Spherical polyacrylamide (PAM) nanoparticles were prepared by inverse emulsion polymerization and were found to have average particle size of 20 nm. In-situ inverse emulsion polymerization of acrylamide in presence of metal oxides nanoparticles ($TiO_2$and ZnO; either individually or in a mixture) was performed. Transmission electron microscope images clearly confirmed the formation of core/shell nanocomposite structure with inner metal oxide core coated with polyacrylamide shell. The composites were further cross-linked to prevent structural deformation in water. The water absorbency of the prepared composites was 1660, 900, 1000 and 700 % for PAM, TiO_2/PAM, ZnO/PAM, TiO2-ZnO/PAM core/shell nanocomposites, respectively.

Water decontamination efficiency of the prepared composites was investigated using organic dyes as models of organic contaminants. The decolorization efficiency of the prepared composites was investigated in dark and under illumination. The nanocomposites showed high ability towards photo-decolorization and especially, the titania nanocomposite showed higher ability towards photo decolorization of Black T and Indigo dyes. A synergetic effect between the adsorption properties of the polymer and the photocatalytic activity of the metal oxides is proposed.

Keywords: Core/shell nanocomposites, Titania nanoparticles, Zinc oxide nanoparticles, Polyacrylamide nanoparticles, Superabsorbent hydrogel, Water treatment, Photocatalytic activity, Adsorption.

1. Introduction

Dyes are an abundant class of colored organic compounds that represent an increasing environmental danger. Most textile dyes are photo-stable and refractory towards chemical oxidation that renders them resistant towards degradation by conventional biochemical and physicochemical methods. Synthetic dyes are being used in textiles, papers, leathers, additives, foodstuffs, cosmetics,

[*] Corresponding author: raniaelsayed@yahoo.com

laser materials, laser printing, etc. As one kind of typical pollutants, synthetic dyes have attracted much attention. Every year, about 280,000 tons of synthetic dyes were discharged into environmental water [1], which causes a severe influence on both environment and human health. Even small amount of dye in water is highly visible, affecting water transparency and gas solubility and consequently reducing the photosynthetic activity in aquatic biota [2]. Some dyes are also highly toxic, carcinogenic and mutagenic and they can even bio-accumulate in food chain [3]. Therefore, it is urgent to develop effective methods for treatment of industrial wastewater containing synthetic dyes.

Metal oxides have been extensively investigated as photo-catalysts due to their stability and non-toxicity. Practically, one of their drawbacks is the recycling of the nano-sized metal oxide powders. Additionally, they exhibits low adsorption ability for the pollutants which has attracted much attention to anchor them on. This problem could be minimized by using the photo-catalyst in immobilized form [4]. The suggested supports should have some advantages, such as low cost and easy separation from the treated solution and should be UV light resistant in order to avoid the UV light catalytic degradation of the organic substrate themselves. Hence, with the progress of the fabrication technique and the exploitation of new composites based on organic substrates, photocatalysts supported on organic substrates have a wide practical application. Some publications have reported that the modified TiO_2 showed better adsorption capacity than the pristine TiO_2 [5,6,7]. Janus et al [5], for example, compared the adsorption capacities of unmodified and carbon modified TiO_2, and found the adsorption ability of TiO_2 was improved at least 10 times by modification. For another example, polypyrrole has been used as a support for TiO_2 in many studies because of its high thermal stability and non-toxicity [8]. In fact, it is recognized that polypyrrolealso has the adsorption ability through ion exchange or electrostatic interaction, largely owing to the existence of positively charged nitrogen atoms in polypyrrolematrix [9,10,11].Therefore, the improvement in the adsorption and regeneration capacities of the photo-catalyst through modification with other materials is highly desired. Accordingly, Novel polymer nanocomposite dispersions based on different kinds of inorganic nanoparticles with further enhanced physical and chemical properties are strongly desired. The enhancement of the physical properties of nanocomposites depends mostly on the homogeneous dispersion of the inorganic nanoparticles. Therefore, the formation and exploitation of new types of polymer nanocomposite with high performance has become a major challenge.

There are many different methods for preparation of inorganic/ polymer nanocomposites; among which are the solution mixing and the in-situ polymerization involving the different

polymerization techniques. Very interestingly, Hu and Chen found in their study on double hydroxide/polyacrylamide nanocomposites that, the aqueous dispersions nanocomposites prepared via in-situ polymerization exhibited further enhancements in physical properties compared to those prepared by solution mixing [12].

Polymer hydrogels are soft materials consisting of a network of hydrophilic polymer with high water content [13]. A unique network microstructure, consisting of a flexaible polymer chains linked by inorganic nanoparticles, contributes to their greatly improved water-swelling properties.

The inverse emulsion polymerization of acrylamide results in spherical nanoparticles of polyacrylamide nanoparticles (PAM.NPs) and upon using dispersed photocatalyst in the polymerization media; it leads to the formation of core of the metal oxide surrounded by a shell of the polymer. The nanoscale production of the polymer particles followed by cross-linking of the polymer can result in a superabsorbent material.

Based on the unique absorbent characters and the network structure of the superabsorbent crosslinked PAM and the excellent photocatalytic degradation activity of TiO_2 and ZnO nanoparticles; in this work, a novel materials; PAM.NPs, TiO2/PAM.NC, ZnO/PAM.NC and TiO2-ZnO/PAM.NC were prepared by cross-linking after in-situ inverse emulsion polymerization in presence and absence of TiO_2, ZnO and their mixture, and their photocatalytic activities were evaluated using different organic dyes as degradable targets.

2. Experimental part

2.1. Materials

Acrylamide monomer was purified by recrystallized from ethanol. Glutraldehyde was used as a crosslinker, Potassium peroxy-disulfate ($K_2S_2O_8$) as a radical initiator and a mixture of span 80 and tween 80 as surfactants. The oil phase of the inverse (water in oil) emulsion polymerization was n-hexane and the aqueous phase was acrylamide dissolved in water. Congo Red (CR), Indigo Carmine (IC) and Eriochrome Black T (EBT) were used as photocatalytic degradation targets. All other reagents were of high grad and were used without further purification.

2.2. Materials preparation

2.2.1.Preparation of TiO_2 nanoparticles

For preparing nanosized TiO_2 powder sol-gel method [14] was used as following: 25 ml of $TiCl_4$ (15%) was dissolved in 20 ml distilled water in an ice-water bath. The solution was slowly mixed with 30 ml distilled water and 20 ml ethanol (dispersing agent). Ammonia was then added dropwisely

until a pH of 9, the solvent was then evaporated at 80°C for 24 h and the formed precipitate was dried at 300°C for 2 h and then calcined in an air stream at 500° C for 4 h.

2.2.2. Preparation of ZnO nanoparticles

Zinc oxide nanoparticles were synthesized by wet chemical method using zinc nitrate and sodium hydroxide precursors [15], a 0.5 M aqueous ethanol solution of zinc nitrate ($Zn(NO_3)_2.4H_2O$) was kept under constant stirring. After complete dissolution of zinc nitrate, 0.9 M NaOH aqueous solution was added under high speed constant stirring, drop by drop (slowly for 45 min) touching the walls of the vessel. The beaker was sealed at this condition for 2 h then the precipitate was filtered and dried in air atmosphere at 60°C. During drying, $Zn(OH)_2$ is completely converted in to ZnO.

2.2.3. Preparation of polyacrylamide nanoparticles (PAM.NPs)

PAM.NPs were prepared via inverse emulsion polymerization [16]. The water phase; Acrylamide monomer (5g) was dissolved in distilled water (7.5ml) at ambient temperature) was dropwisely added to the oil phase (n-hexane containing the surfactant mixture of 0.665 gram of span 80 and 0.33 gram of tween 80 at 40°C under continues stirring unit complete emulsification of the system which indicated from the complete mixing of the two phases and the formation of milk like homogeneous solution. The system was then degassed under vacuum for about 30 minutes after which the initiator (0.0625 gram of AIBN) was added as a one portion and the temperature was raised to 80°C under a nitrogen atmosphere. After completion of the polymerization reaction, the mixture was washed with excess n-hexane and then with ethanol to remove any impurities, filtered and dried under vacuum at 80°C to constant weight and milled, thus a powdered product has been denoted as PAM.NPs.

2.2.4.Preparation of metal oxide/PAM (core/ shell) nanocomposites

Metal oxide/ PAM (core/ shell) nanocomposites were synthesized by in-situ inverse emulsion polymerization method. A predetermined amount (5% of the total weight) of TiO_2nano-powder, ZnOnano-powder or their mixture was dispersed in the surfactant solution and sonicated for 20 minutes for homogenous dispersion. The inverse emulsion polymerization was then carried out as mentioned in the previous section. The products are abbreviated as TiO_2/PAM.NC nanocomposite, ZnO/PAM.NC or TiO_2-ZnO/PAM.NC.

2.3. Crosslinking of polymer nanoparticles and nanocomposites

The prepared nanocomposites were crosslinked by reflux in 10:90 of Gluteraldehyde and ethanol, respectively for 2 hours and then filtrated, washed extensively with ethanol and dried under vacuum at 80° C to constant weight.

2.4. Materials characterizations

For characterization of the prepared materials, average particles size, particles size distribution and zeta potential were measured using Dynamic light scattering (Malvern-ZS nano-series). Transmission electron microscopy (JEOL-2100F) was used and digital photography was performed. The crystalline structure was investigated via X-ray diffraction analysis (XRD) using Shimadzu XD-1 diffractometer.The phase identification was made according to the Joint Committee on Nanoparticles Diffraction Standards (JCPDS). The crystallite size, D_{XRD} was calculated according to Scherer equation [17]. The textural properties were followed up using the N_2 adsorption desorption isotherms measured at liquid nitrogen temperature (-196°C) using NOVA-2000 gas sorption analyzer (Quantachrome Corp. system).

2.5. Water absorbency

One gram of TiO_2/PAM.NC, ZnO/PAM.NC and TiO_2-ZnO/PAM.NC were immersed in water for the absorption of water into the network of the composite and the formation of a hydrogel. The un-adsorbed water was removed by filtration and the hydrogels were hanging for few minutes. The hydrogel was weighted at different time intervals till reach water absorption equilibrium. The water uptake capacity was calculated by the following formula:

$$\text{water absorbency\%} = {}^{(W_t - W_0)}/_{W_0} * 100\%$$

where W_t is weight of hydrogel at time t and W_0 is the initial weight of the polymer nanoparticles or nanocomposites.

2.6. Photocatalytic experiments

The desired weight of the nanocomposite was primary soaked in water 24 hour before performing the experiment to form the hydrogel. The photocatalytic experiment was carried out in a cylindrical Pyrex reactor, containing 300 mL of the 25 ppm dye solution with the desired amount of the nanocomposite on a magnetic stirrer set at 300 rpm to maintain the nanocomposite in suspension. The suspension was irradiated with UV 254 nm (8 W) pen-ray lamp. All experiments were performed at 25± 1°C. In order to monitor the dye concentration in the solution, a 10 ml aliquot was analyzed using a JENWAY-6505 UV-visible spectrophotometer (at λ_{max}= 410 nm for EBT, 496 nm for CR and 608 nm for IC) at the appropriate time intervals.

3. Results and discussion

3.1. Metal oxides nanoparticles photocatalysts

TiO_2 and ZnO were prepared by sol-gel and wet-chemical methods; respectively and were characterized using TEM, DLS and XRD. The results were summarized in Table 1 and shown in Figure 1 and 2. The prepared TiO_2 nanoparticles were found to be a mixture of anatase and rutile [JCPDS card 00-001-1292], as detected by XRD analysis. The average particles size was around 15 nm as determined from the TEM images while the DLS average size was 206 nm and the Zeta potential value was -18 mV. The samples were shown significantly large mean particle size by DLS analysis, compared with TEM analysis, because these samples are present in aggregates state in the solution but the TEM analysis provides more authentic results. DLS analysis may be more efficient method available for colloid particle size determination but TEM is more reasonable if it is concerned to determine the primary particle size [18]. In our case, the difference in the particles sizes for the same sample using different characterization techniques can be attributed to that TEM depends mainly on imaging so one can take the exact dimensions of individual particles while DLS (which depends to a large extent on the preparation condition and solvent interactions) identify aggregates so it can measure an aggregate of particles as one identity.

For ZnO; the diffraction peaks was in accordance with the standard hexagonal zincite phase of ZnO[JCPDS card 01-078-3315]. The average particles size was around 35 nm as determined from the TEM images while the DLS average size was 266 nm and the zeta potential value was -6.9 mV.

Table 1: Summarization of the physical characteristics of the prepared photocatalysts

Photo-catalyst	**Mean crystallite size (from TEM) (nm)**	**Mean nanoparticle size(nm)(from Zetasizer Nano ZS)**	**S_{BET} (m^2/g)**	**Pore radius (nm)**	**Pore volume (cc/gm)**	**Z-Zeta Potential (mV)**	**Z- Zeta Potential for polymer (mV)**
TiO_2	14.48	206	45.59	6.24	0.213	-18	-885
ZnO	34.51	266	8.63	1.232	0.020	-6.9	-246
TiO_2-ZnO	------	--------	31.75	8.808	0.128	------	-210

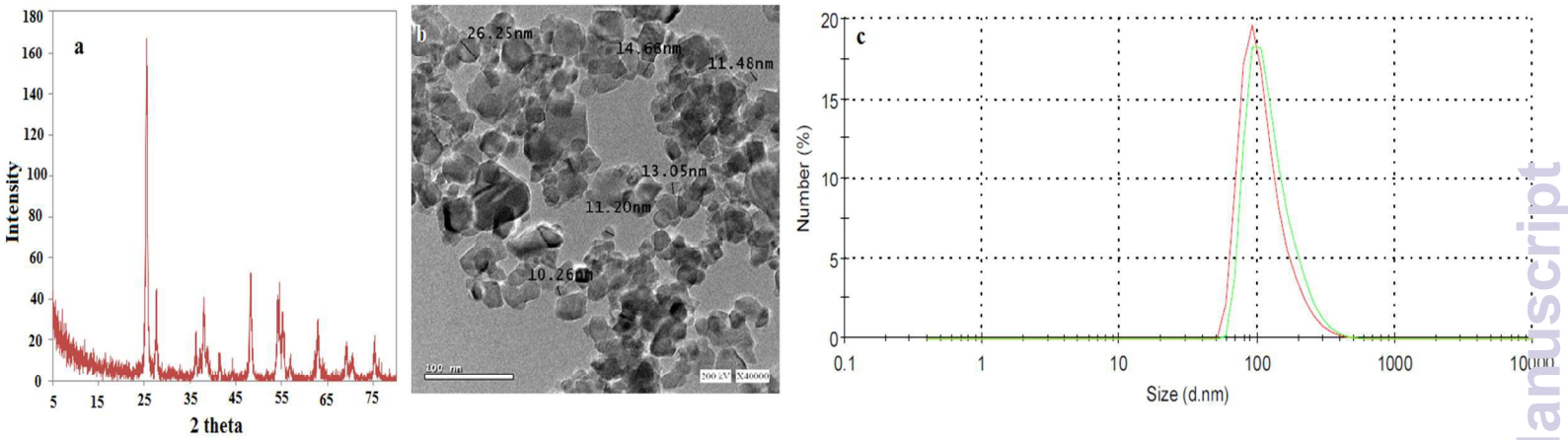

Figure 1: Characteristics of the prepared TiO_2NPs; (a) XRD, (b) TEM and (c) DLS measurements

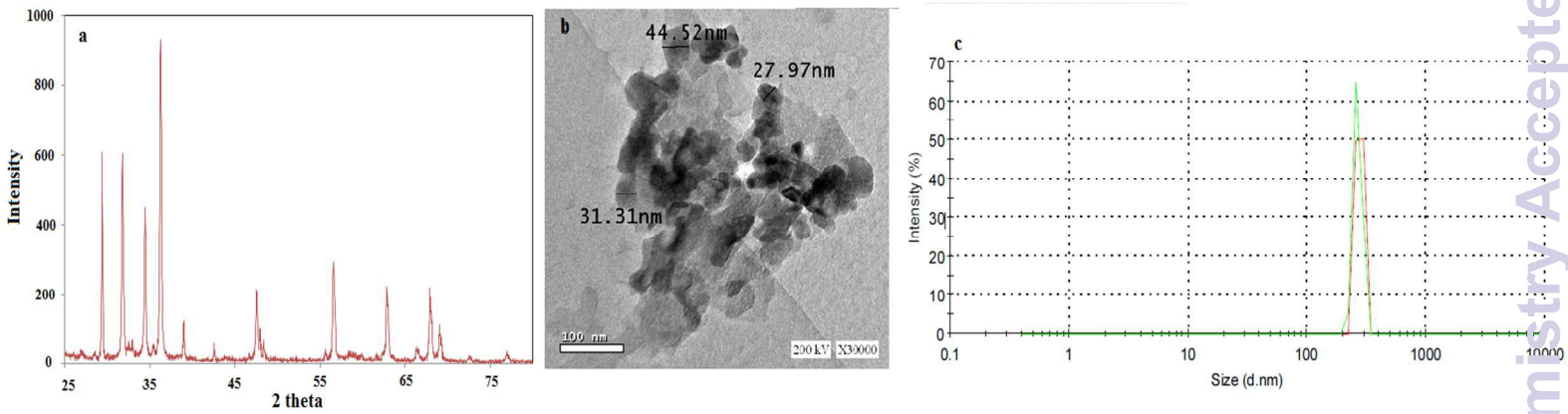

Figure 2: Characteristics of the prepared ZnO NPs; (a) XRD, (b) TEM and (c) DLS measurements

TiO_2 spectrum (see Figure 3) shows a broad band at 3401cm^{-1} which can be assigned to the stretching vibration of physically bonded hydroxyl groups (O–H). The band at 1625 cm^{-1} can be assigned to bending mode of hydroxyl groups or deformation vibrations of adsorbed water molecules [19]. The band at ~ 690 cm^{-1} corresponds to the Ti–O–Ti stretching vibration in crystal TiO_2 [20]. In the FT-IR absorption spectrum of ZnO nanoparticles, the peak at 470 cm^{-1} is the characteristic absorption of Zn–O bond and the broad absorption peak at 1638 $cm^{-1}$and 3487 cm^{-1}indicate the presence of –OH and C=O residues, probably due to atmospheric moisture and CO_2 respectively [21]. The FT-IR spectrum of the TiO_2-ZnO composite showed all bands characteristic to TiO_2 and ZnO parent material as shown in Fig.3. The bands in the range 3469 cm^{-1} is due to the stretching vibration of O–H bonds in M–OH and the HO–H of water molecules adsorbed on the materials surface due to moisture [22]. The band at 1625 cm^{-1} can be assigned to bending mode of hydroxyl groups or

deformation vibrations of adsorbed water molecules [23]. These are crucial to the photocatalytic reactions since they can react with photo-excited holes generated on the catalyst surface and produce hydroxyl radicals [20].

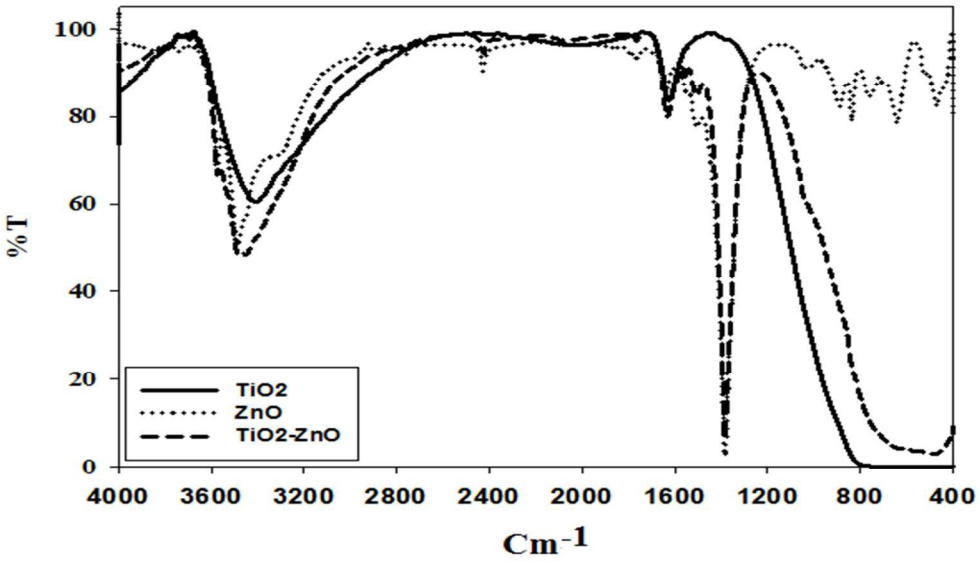

Figure 3: FTIR spectra of TiO_2, ZnO and TiO_2-ZnO nanoparticles

3.2. Polyacrylamide nanoparticles (PAM.NPs)

The TEM image shows spherical nanoparticles of PAM prepared by inverse emulsion polymerization. In this technique, the polymerization process takes place inside the micelles so that the produced polymer particles was as small as micelles size which is usually in the nanoscale and are usually identical with uniform size and shape, as shown in figure 4.

The FT-IR spectrum, figure 4, shows characteristic peaks of PAM; peak at about 1170 cm^{-1} is for $–NH_2$ bending vibration, the small peak at about 1450 cm^{-1} is for the C-N stretching vibration, the peak at 1670 cm^{-1} is belonging to C=O stretching vibration while other peaks (for CH_2- stretching vibration at 2950 $cm^{-1,}$ N-H bending vibration at 3190 cm^{-1}, and O-H stretching vibration at 3462 cm^{-1}) are overlapped in the range of 3200 to 3600 cm^{-1}

Crosslinking of the produced polymer was carried out not only to prevent structure deformation upon interaction with water, but also to get the hydogel property of the cross-linked PAM.NPs. Superabsorbent polymers are a cross-linked hydrophilic polymer with a network structure, which is able to absorb hundreds to thousands times water of its mass to form a hydrogel and they can also integrate with other compounds and network structure to form a stable composite. The swelling performance of crosslinked PAM nanoparticles is shown in figure 4 where the equilibrium reached

within two hours with increase up to 1650% of its original weight. This huge water uptake capacity can be attributed to the nanosize, spherical shape, crosslinking and chemical structure of PAM nanoparticles. Based on the unique absorbent characters and the network structure of PAM, the crosslinked hydrophilic network of PAM nanoparticles can be considered as a superabsorbent polymer.

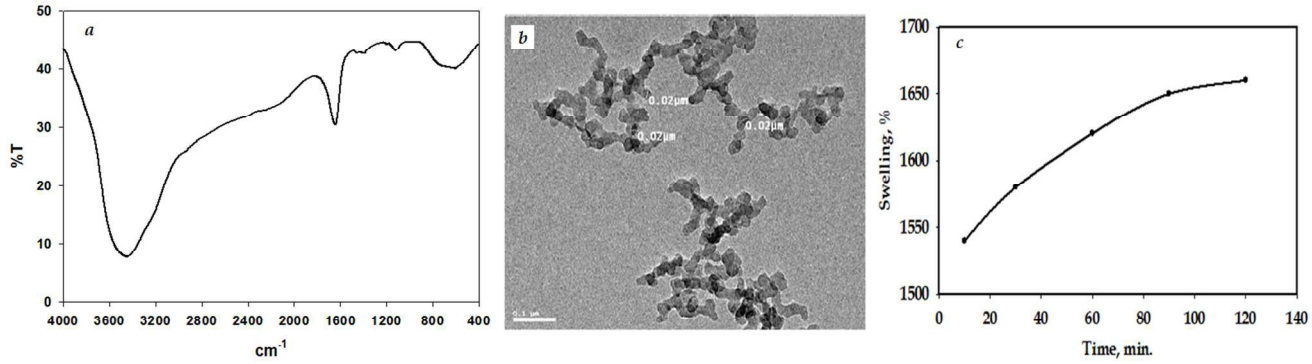

Figure 4: FT-IR of PAM.NPs (a), TEM of PAM.NPs (b) of and water uptake capacity of crosslinked PAM.NPs (c)

3.3. Core/shell (Metal oxide/ PAM nanoparticles)nanocomposites

Practically, catalytic nanoparticles have several drawbacks related to the recycling of the nano-sized fine powders and the low adsorption ability for the pollutants. Hence, photocatalysts supported on polymeric substrates has attracted much attention for a wider practical application.

Metal oxide/PAM core/shell nanocomposite was obtained by in-situ inverse emulsion polymerization method using TiO_2 and ZnO nanoparticles individually and in a mixture as functional cores as schematically represented in figure 5. The inverse emulsion polymerization of acrylamide results in spherical nanoparticles while core/shell structure of the composites was obtained in case of the presence of metal oxide nanoparticles during the polymerization process which leads to the formation of a core of the metal oxide nanoparticles surrounded by a shell of the polymer. The nanoscale production of the PAM particles incorporated with catalytic nanoparticles followed by cross-linking of the polymer can result in a multifunctional (support, super-adsorbent hydrogel) material.

A drastic negative shift in zeta potential of TiO_2 (see table 1) was observed most probably due to the interaction between thePAM.NPs and the surface of photocatalyst was seen when highly adsorbed organic compounds were formed or/and adsorbed on the photocatalysts surface [24].

The presence of the metal oxide nanoparticles inside the crosslinked polymer nanoparticles network was found to decrease the amount of water absorbed leading to decrease the hydogel content

of the polymer nanocomposites as shown in figure 6. This may be attributed to that the metal oxide nanoparticles may act as a connection center inside the polymer matrix which tetrad the diffusion of water inside the polymer network and thus decrease the swelling or the amount of water uptake as schematically represented in the insertion of figure 6.

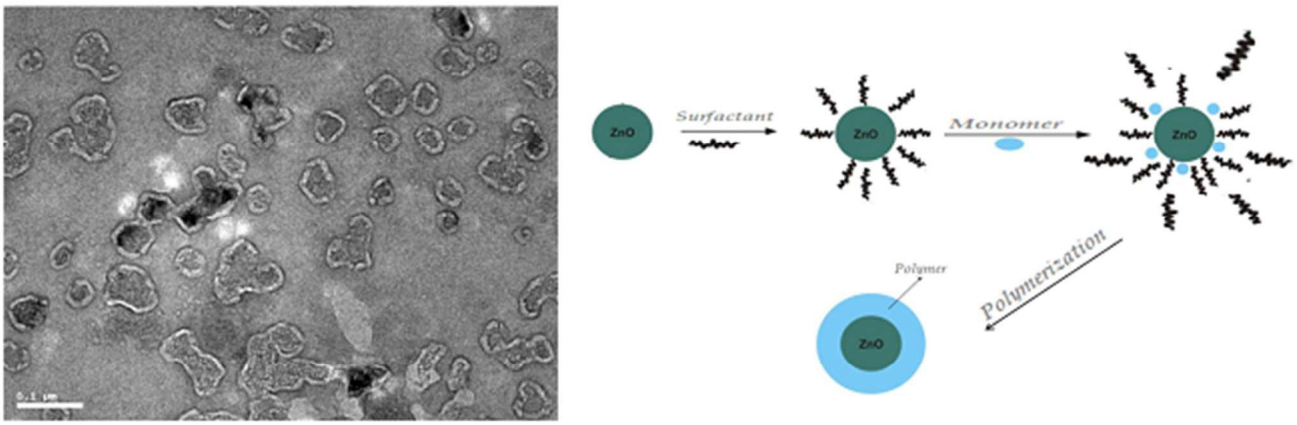

Figure 5: TEM image of the ZnO/PAM core/shell nanocomposite and schematic representation of the suggested core/shell formation mechanism

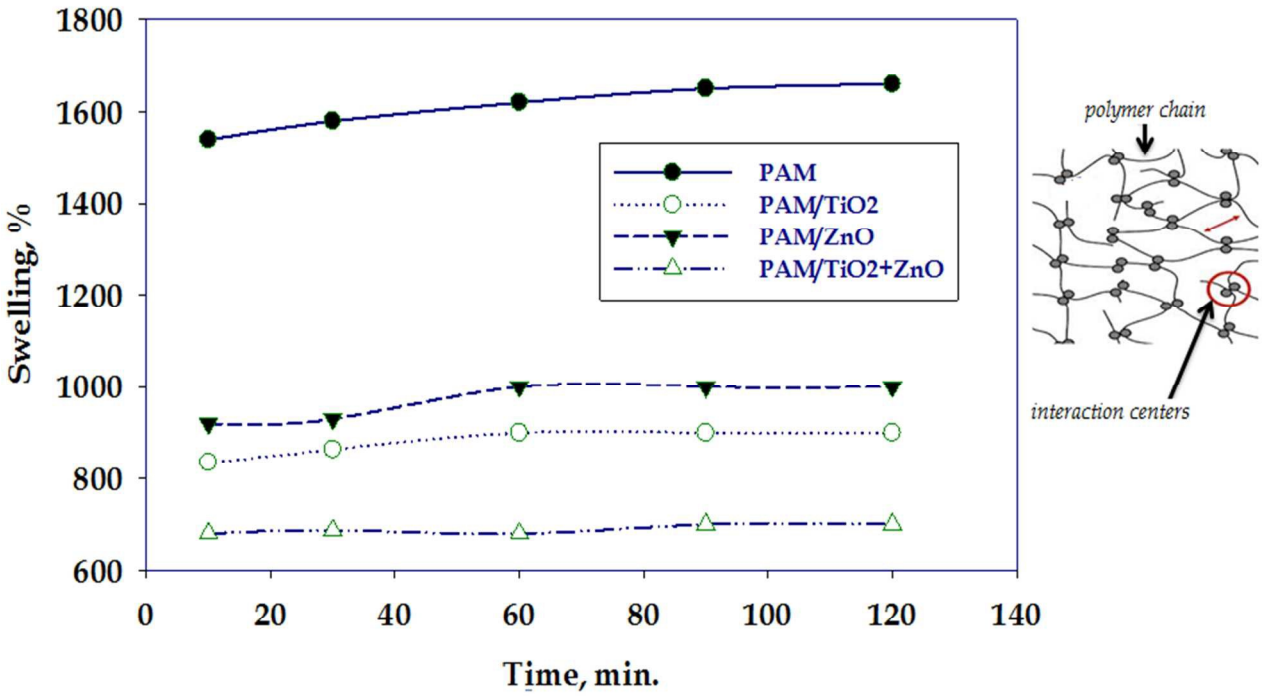

Figure 6: water uptake capacity of crosslinked nanocomposites

3.4. Photocatalytic activity

Synthetic dyes,as a typical kind of dangerous water pollutants, causes a severe influence on both environment and human health; therefore, it is urgent to develop effective methods for their treatment. Titanium dioxide nanoparticles have been extensively studied for degradation of organic pollutants [25,26,27].Further investigations have shown that ZnO may have a similar efficiency of photocatalytic degradation and moreover it could be a better substitution toTiO_2 in some applications [28,29].For semiconductors, illumination promotes the electrons to the conduction band, leaving holes in the valence band producing potential reducing and oxidizing agents. In addition and as observed in the FT-IR spectra of the prepared metal oxides nanoparticles (figure 3), the presence of –OH; M–OH and HO–H of water molecules adsorbed on the metal oxides nanoparticles surface are crucial to the photocatalytic reactions.

Practically, the recycling of the nano-sized powders and the low adsorption ability for the pollutants are of their drawbacks. Supporting on polymeric substrates is highly recommended for a wider practical application. PMA can be considered as a potential supporting material to improve the adsorption and removal efficiency of photo-catalyst powder in addition to its role in the adsorption of the pollutant which increases the probability of interaction between the catalyst and the pollutant. To demonstrate the potential applications of the prepared TiO_2/PAM, ZnO/PAM and TiO_2-ZnO/PAM nanocomposites in waste water treatment, their photocatalytic activities in the decolorization of EBT, IC and CR dyes have been investigated and their activity has been compared with pure TiO_2, ZnO and TiO_2-ZnOnanoparticles. In general; the presence of PAM in the nanocomposites increases adsorption capacity for dyes due to the hydrophilic ability of the crosslinked polymer composites. The adsorption efficiency was generally enhanced in case of the core/shell polymer composite than in case of the individual catalyst for EBT and CR dyes but in case of IC the presence of polymer has no effect on the adsorption efficiency but decrees the catalyst adsorption activity, most properly by shielding between the photo-catalyst and the dye due to the chemical structure of the dye molecules as will be shown later in figure 8. The adsorption % of dyes using nanocomposites after 1h in the dark is represented in Table 2.

Table 2: Adsorption effeciency of EBT, CR and IC dyes using TiO_2, ZnO and their mixture individually and as core/shell nanocomposites after 1h in dark

Materials / Dyes	Adsorption %		
	EBT	**CR**	**IC**
TiO_2	11.24	24.84	27.92
PAM/TiO_2	31	92.36	22.28

ZnO	0	25.64	24.08
PAM/ZnO	65.48	95.24	3.7
TiO_2-ZnO	0	81.48	34.72
PAM/TiO_2+ZnO	24.38	86.4	0

The photocatalytic efficiency derived from the changes of organic dyes concentration can be represented by the dye concentration relative ratio C/C_o. Figure 7 (left) shows the photo-degradation of EBT dye using TiO_2, ZnO and TiO_2-ZnO nano-composites. Obviously, the results showed that TiO_2 nanoparticles possess the highest activity for EBT dye degradation. The order of degradation rate was TiO_2 (28%) >ZnO (20%) >TiO_2-ZnO (4%). This attributed to the higher surface area and zeta potential of TiO_2; as illustrated in Table 1. A large surface area of nanoparticles promotes adsorption, desorption and diffusion processes, which is favorable for high photocatalytic activity [30,31]. Figure 7 (right) shows the photo-degradation of EBT dye using TiO_2/PAM, ZnO/PAM and TiO_2-ZnO/PAM hydrogel nanocomposites. The order of degradation rate was TiO_2/PAM (58%) >ZnO/PAM (28%) > TiO_2-ZnO/PAM (22%). The activity of TiO_2/PAM is twice higher than pure $TiO_2$and it is higher by 5.5 times for TiO_2-ZnO/PAM than TiO_2-ZnO due to high increase in zeta potential value and thus the adsorption capacity upon incorporation of the catalyst nanoparticles in a polymer nanoparticles. In the case of CR dye, the adsorption efficiency increase significantly by incorporating the nanoparticles into the polymer nanoparticles forming the core/shell nanocomposites; as illustrated in Table 2.Under illumination and when the illumination time is extended to 180 min, the color of CR solution nearly disappeared completely; the photocatalytic degradation rate of CR is (96%) for ZnO/PAM > (94%) for TiO_2-ZnO/PAM >(89%) for TiO_2/PAM. This attributed to the highest ability to water uptake of ZnO/PAMnanocomposite comparison to other one, as shown in Figure 6.This increases the contact between dye molecules and photocatalyst which decrease the ability of e^-/h^+ recombination over ZnO. The adsorption efficiency for the IC dye, as shown in Table 2, does not affected mostly by the presence of polymer shell in case of TiO_2/PAM but in case of ZnO/PAM and TiO_2-ZnO/PAM nanocomposites, the adsorption efficiency decreased significantly. Here, it seems to include lower electrostatic interaction between the network of hydrogel containing ZnO, which has more hydroxyl radicals on its surfaces as indicated from their sharp peak on the FT-IR spectra (figure 3), and dye macromolecule which negatively affects the adsorption process [32]. Under illumination, the decolorization efficiency of TiO_2/PAM nanocomposite further increased compared with pure catalyst from about 42% to 68% while for ZnO the decolorization efficiency decreased significantly from 70% to 25 % in ZnO/PAM

and from 85% to 83% in case of TiO_2-ZnO/PAM, most probably due to the decrease in the primary adsorption process.

Generally, there are many factors that may influence the adsorption of the dye such as surface charge and structure of the dye, adsorbent surface properties, hydrophobic and hydrophilic nature, hydrogen bonding, electrostatic interaction, steric effect, van der Waals forces, and so forth [33]. A Correlation between the photocatalytic activities of the prepared core/shell nanocomposites with some of their physical properties is represented in figure 8.

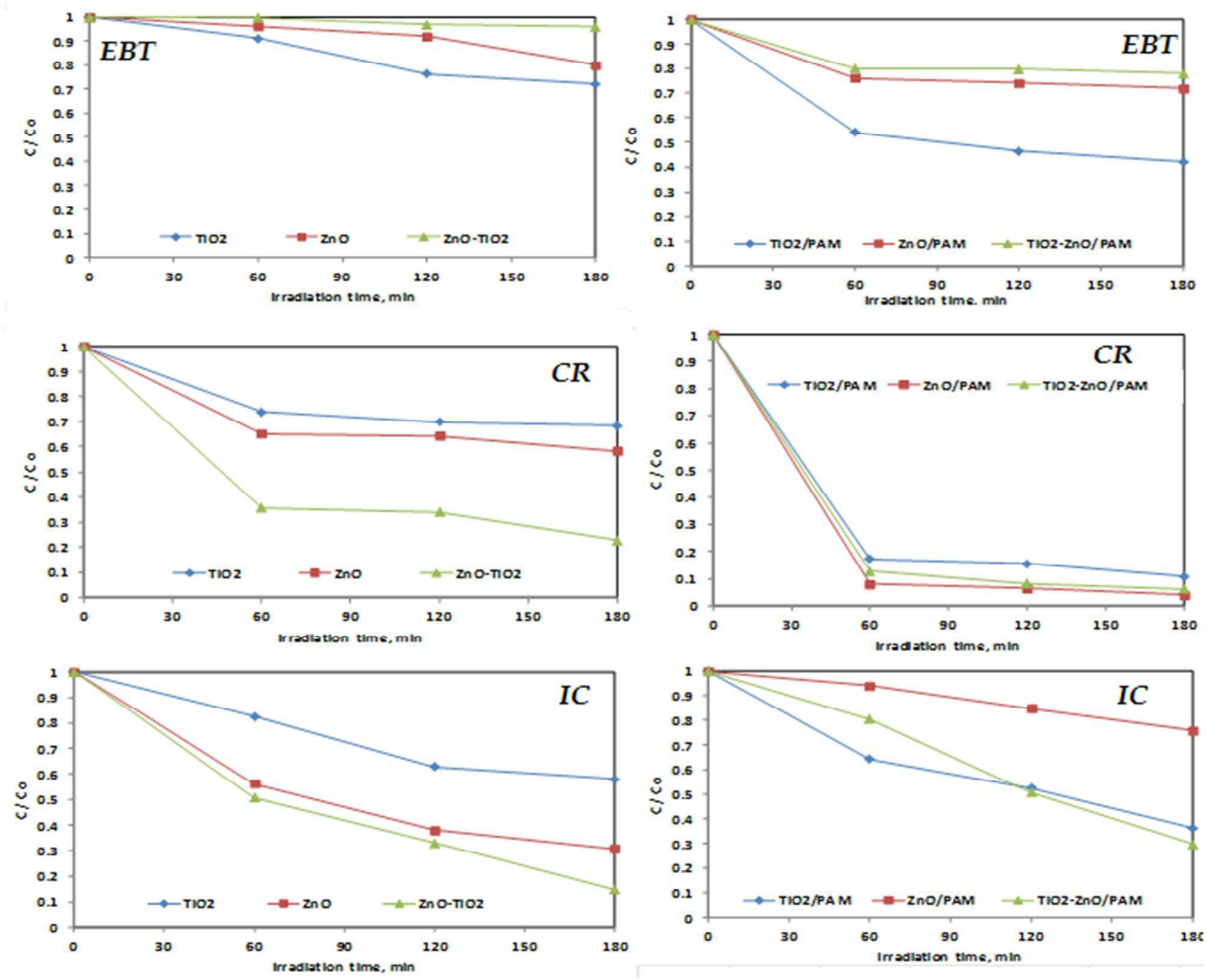

Figure 7: Photo-degradation of EBT dye using TiO2, ZnO and TiO2-ZnO in pure form (left) and in the core/shell composite form (right).

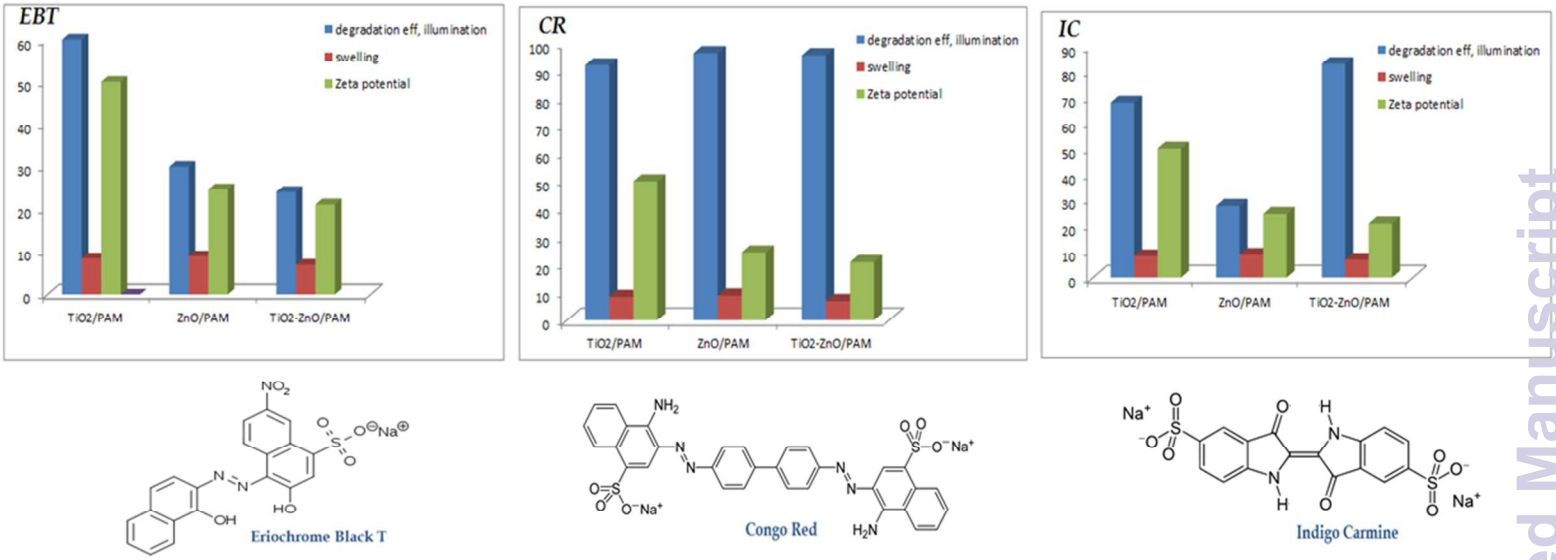

Figure 8: Correlation of the Photocatalytic activity of the prepared core/shell nanocomposites with some of their physical properties

4. Conclusion

Spherical polyacrylamide nanoparticles (PAM.NPs), prepared by inverse emulsion polymerization, were found to have average particle size of 20 nm. In-situ inverse emulsion polymerization of acrylamide, in presence of metal oxides nanoparticles (TiO_2 and ZnO; either individually or in a mixture), results in the formation of core/shell nanocomposite structure with inner metal oxide core coated with PAM shell. The composites were further cross-linked to prevent structural deformation in water. The water absorbency of the prepared composite was 1660, 900, 1000 and 700 % for PAM, TiO_2/PAM, ZnO/PAM, TiO2-ZnO/PAM core/shell nanocomposites, respectively. The decolorization efficiency of the prepared composites was investigated in dark and under illumination revealing that the nanocomposites showed high ability towards photo-decolonization and especially, the titania nanocomposite which showed higher ability towards photo decolonization of Black T and Indigo dyes. A synergetic effect between the adsorption properties of the polymer and the photocatalytic activity of the metal oxides is proposed.

References

[1] S. Chowdhury and R. Balasubramanian, *Appl. Catal., B.,* 2014, **160-161**, 307-324.

[2] Z. Zhang, R. Y. Yang, Y. S. Gao, Y. F. Zhao, J. Y. Wang, L. Huang, J. Guo, T. T. Zhou, P. Lu, Z. H. Guo and Q. Wang, *Scientific Reports,* 2014, **4,** 6797-6809.

[3] H. S. Rai, M. S. Bhattacharyya, J. Singh, T. K. Bansal, P. Vats and U. C. Banerjee, *Environ. Sci. Technol.,* 2005, **35**, 219-238.

[4] N. M. Mahmoodi and M. Arami, *J. Appl. Polym. Sci.,* 2008, **109**, 4043-4048.

[5] M. Janus, E. Kusiak, J. Choina, J. Ziebro and A. W. Morawski, *Desalin.*, 2009, **249,** 359–363.

[6] M. Janus, J. Choina and A. W. Morawski, *J. Hazard. Mater.,* 2009,**166,** 1–5.

[7] D. W. Bahnemann, S. N. Kholuiskaya, R. Dillert, A. I. Kulak and A. I. Kokorin, *Appl. Catal., B.*, 2002, **36,** 161- 169.

[8] X. Zhang and R. B. Bai, *J. Mater. Chem.,* 2002, **12**, 2733–2739.

[9] X. Zhang, R. B. Bai and Y. W. Tong, *Sep. Purif. Technol.,* 2006, **52,** 161–169.

[10] S. K. Bajpai, V. K. Rohit and M. Namdeo, *J. Appl. Polym. Sci.,* 2009, **111**, 3081–3088.

[11] M. Karthikeyan, K. K. Satheeshkumar and K. P. Elango, *J. Hazard. Mater.,* 2009, **167,** 300–305.

[12] Z. Hu and G. Chen*, J. Mater. Chem. A*, 2014, **2**, 13593–13601.

[13] Z. Hu and G. Chen, *Adv. Mater.,* 2014, **26**, 5950–5956.

[14] S. A. Hassan and R. A. El-Salamony; *Canadian Chemical Transactions,* 2014, **2,** 56-70.

[15] S. Talam, S. R. Karumuri and N. Gunnam, *International Scholarly Research Network ISRN Nanotechnology* Volume 2012, Article ID 372505, doi:10.5402/2012/372505.

[16] B. Kriwet, E. Walter and T. Kissel, *J. Controlled Release,* 1998, **56,** 149–158.

[17] R. Elsalamony and D. Abd El-Hafiz; *Chem. Mater. Res.*, 2014, **6,** 122-134.

[18] D. Lee, G. Cho, H. Lim, D. Kim, C. Kim and S. Lee*, J. Ceram. Process. Res.,* 2013, **14**, 274-278.

[19] C. Xie, Z. L. Xu, Q. J. Yang, B. Y. Xue, Y.G. Du and J. H. Zhang, *Mater. Sci. Eng.: B,* 2004, **112**, 34-41.

[20] T. C. Jagadale, S. P. Takale, R. S. Sonawane, H. M. Joshi, S. I. Patil, B. B. Kale and S. B. Ogale, *J. Phys. Chem. B,* 2008, **112**, 14595-14602.

[21] V. Parthasarathi and G. Thilagavathi, *Int. J. Pharm. Pharm. Sci.*, 2011, **3**, 392-398.

[22] F. Adam and H. K. Fua, *Malaysian Patent,* 2008, MY-136715-A.

[23] C. Xie, Z. L. Xu, Q. J. Yang, B. Y. Xue, Y. G. Du and J. H. Zhang, *Mater. Sci. Eng. B,* 2004, **112**, 34-41.

[24] S. W. Lam, K. Chiang, T. M. Lim, R. Amala and G. Low; *J. Photochem. Photobiol., A,* 2007, **187,** 127–132.

[25] A. Mills and S. L. Hunte, An overview of semiconductor photocatalysis, *J. Photochem. Photobiol., A,* 1997, **108**, 1–35.

[26] H. Fu, L. Jing, Y. Qu, B. Wang, S. Li, B. Jiang, L. Yang and W. Fu, *Sol. Energy Mater. Sol. Cells,* 2006, **90**, 1773–1787.

[27] I. K. Konstantinou and T. A. Albanis, *Appl. Catal., B,* 2004, **49,** 1–14.

[28] A. M. Abdulkarem, E. M. Elssfah, Y. Nan-Nan, G. Demissie and Y. Ying*., J. Phys. Chem. Solids,* 2013, **74**, 647–652.

[29] X. Cai, Y. Cai, Y. Liu, H. Li, F. Zhang and Y. Wang, *J. Phys. Chem. Solids,* 2013, **74**, 1196–203.

[30] C. Xu, X. Wei, Z. Ren, Y. Wang, G. Xu, G. Shen and G. Han, *Mater. Lett.,* 2009, **63,** 2194–2197.

[31] N. Venkatachalam, M. Palanichamy and V. Murugesan, *Mater. Chem. Phys.,* 2007, **104,** 454–459.

[32] L. G. Devi and S. G. Kumar, *Appl. Surf. Sci.,* 2011, **257**, 2779–2790.

[33] M. Li, H. Wang, S. Wu, F. Liand and P. Zhi, *RSC Adv.*, 2012, **2**, 900–907.